Electron Spin Resonance Study of the Binding Structures of Cationic Water-soluble Metalloporphyrins on Highly Oriented Deoxyribonucleic Acid Fibres

Makoto Chikira,*[a] Shoichi Suda,[a] Toyotaka Nakabayashi,[a] Yoshihito Fujiwara,[a] Takashi Ejiri,[a] Mitsuhide Yoshikawa,[a] Nagao Kobayashi[b] and Heisaburo Shindo[c]

[a] *Department of Applied Chemistry, Chuo University, 1-13-27, Kasuga, Bunkyo-ku, Tokyo 112, Japan*

[b] *Pharmaceutical Institute, Tohoku University, Aramaki, Sendai 980, Japan*

[c] *Tokyo College of Pharmacy, 1432–1, Horinouchi, Hachioji, Tokyo 192-03, Japan*

The binding structures of several paramagnetic metal complexes of 5,10,15,20-tetrakis(1-methyl-4- or -2-pyridinio)porphyrin (H_2L^1 or H_2L^2) on the highly oriented DNA fibres were investigated by means of ESR spectroscopy and computer simulations of the spectra. The structural parameters characteristic of the sterospecific groove binding were obtained for $[CuL^2]Cl_4$, high-spin $[FeCl(L^1)]Cl_4$ and low-spin $[CoL^1][ClO_4]_4$ and the low-spin monoimidazole adduct $[CoL^1(Him)][ClO_4]_4$. They bind to the DNA with the normals of the porphyrin planes tilted by about 45° from the double helix axes. The low-spin bis(imidazole) adduct $[FeCl(L^1)(Him)_2]Cl_4$ binds to A-form DNA with the porphyrin plane nearly parallel to the double helix axis. The complex $[CoL^1][ClO_4]_4$ binds to DNA as an intercalator as well as a groove binder. It was also revealed that some metalloporphyrins stabilize the tertiary structures of DNA around the binding sites.

The interaction of water-soluble porphyrins with DNA has been a subject of intense investigation.[1–24] Some porphyrins induce photosensitive reactions and some metalloporphyrins can make dioxygen highly reactive, triggering various oxygenation reactions in biological systems.[25,26] It has been reported that complexes of Cu^{II} and Ni^{II} of the cationic porphyrin 5,10,15,20-tetrakis(1-methyl-4-pyridinio)porphyrin, (H_2L^1) bind intercalatively to GC-rich regions in a DNA double helix, while those of Fe^{III}, Mn^{III}, Co^{III} and Zn^{II} bind non-intercalatively to AT-rich regions.[1,2,4] The difference in the binding mode has been attributed to the difference in the co-ordination at the apical positions of the metalloporphyrins, *i.e.* the complexes of Cu^{II} and Ni^{II} have weakly bound axial ligands while the others have strongly bound ones which interfere with the intercalative binding of the complexes. The positions of the *N*-methyl groups also affect the binding. In the case of 5,10,15,20-tetrakis(1-methyl-2-pyridinio)porphyrin (H_2L^2), the *N*-methyl *ortho*-substituents disrupt sterically the intercalation and force the porphyrin complexes to bind on the surface of the DNA double helix.[4]

Ward *et al.*[10,11] based on a footprinting technique suggested that the complexes of Fe^{III}, Mn^{III}, Co^{III} and Zn^{II} bind to the AT-rich minor groove of the DNA. Marzilli and co-workers[12–17] extensively investigated the interaction of water-soluble porphyrins with DNA using a variety of physical techniques: viscosity, flow dichroism, NMR and electron nuclear double resonance (ENDOR). They reported that derivatives with bulky *N*-alkyl substituents such as propyl or 2-hydroxyethyl groups intercalate to DNA.[17] Nakamoto and co-workers[18–20] reported resonance-Raman studies of the interaction of complexes of Cu^{II}, Ni^{II} and Co^{III} of H_2L^1 and its structural analogues with calf thymus DNA, with some polydeoxynucleotides and with several hexadeoxyribonucleotides. They found bands characteristic of intercalation, groove binding and coulombic interaction respectively, and proposed two different non-intercalative binding modes, a groove binding and an electrostatic outside binding. Recently, Kuroda *et al.*[21] reported an induced CD study of the binding mode of the porphyrins and biochemical studies of the sequence-specific recognition of DNA.

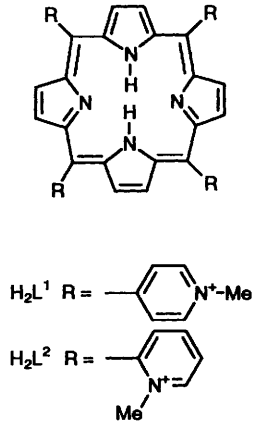

Despite all the above experimental results, the geometrical parameters which characterize the binding mode of the porphyrins have scarcely been reported particularly for the groove- or outside-bound porphyrins except for the zinc complex of H_2L^1.[22] Recently, we demonstrated that the ESR spectroscopy of the paramagnetic metal complexes on DNA fibres is a powerful technique to address these problems.[27–30] To establish the geometry of the metalloporphyrins bound non-intercalatively to DNA, we measured the ESR spectra of several paramagnetic metal complexes of the water-soluble porphyrins H_2L^1 and H_2L^2 on salmon sperm DNA fibres. It is well known that the axes of the DNA double helices in carefully fabricated DNA fibres are almost parallel to the elongation direction of the fibres.[31] If a paramagnetic metalloporphyrin has a specific orientation in the fibre, the ESR line shape of the complex varies with the direction of the fibre axis in the static magnetic field. The simulations of the orientation-dependent ESR spectra will give an average angle between the normal of the porphyrin plane and the DNA double helix axis as well as the standard deviation of the angle fluctuation. From the estimated angle and its deviation, we can easily distinguish stereospecific

from non-stereospecific binding or intercalative from non-intercalative binding.

Experimental

Materials.—The complexes $[CuL^1]Cl_4$ **1**, $[CuL^2]Cl_4$ **2**, $[FeCl(L^1)]Cl_4$ **3** and $[CoL^1][ClO_4]_4$ **5** were synthesized as previously described.[32-34] Salmon-sperm DNA was obtained from Pharmacia. The other reagents were all reagent grade used without further purification.

Preparation of DNA Fibres.—Salmon-sperm DNA (100 mg) was dissolved by stirring gently in 40 cm^3 of 10 mmol dm^{-3} Tris·HCl [Tris = tris(hydroxymethyl)methylamine] and 1 mmol dm^{-3} edta (ethylenediaminetetraacetate) solution (pH 7.4–7.5) at 4 °C for about 24 h. The DNA was precipitated by ethanol, collected with glass rods and washed with a 60% aqueous ethanol solution. After being dried at room temperature, the DNA was dissolved in 10 mmol dm^{-3} NaCl solution (40 cm^3) and centrifuged at 30 000 × *g* for 90 min to remove undissolved material. The concentration of the DNA was monitored by the UV absorption at 260 nm (ε = 1.30 × 10^4 dm^3 mol^{-1} cm^{-1} per base pair).

To this DNA solution a metalloporphyrin solution (2 × 10^{-5} mol dm^{-3}) was added very slowly to make the ratio of the porphyrins to base pair about 1:20 for complexes of Cu^{II}, Co^{II} and low-spin Fe^{III} and about 1:50 for high-spin Fe^{III}. Addition of a small amount of sucrose to the porphyrin solution was useful to prevent the oxidation of $[CoL^1][ClO_4]_4$ **5**. An excess of imidazole was added to the DNA solution before the addition of $[FeCl(L^1)]Cl_4$ **3** or after the addition of **5** respectively, to make DNA fibres bound to imidazole-adduct porphyrins. The orders of mixing the imidazole solution were important to prevent precipitation of the DNA by added **3** or oxidation of **5** by the oxygen remaining in the system.

After equilibrating the mixed solution for 1 h, it was ultracentrifuged at 320 000 × *g* for 8 h; the resulting DNA pellet was used to make oriented DNA fibres. A drop from a pellet was suspended and dried at 4 °C for about 24 h between two heads of toothpicks fixed 4 mm apart from each other. In the case of **5** and $[Co(L^1)(Him)][ClO_4]_4$ **6** (Him = imidazole), all the manipulations were undertaken under an atmosphere of nitrogen using Schlenk-type reaction vessels or a glove-box. Once complex **5** was bound to the DNA it was fairly stable under atmospheric oxygen for a long period, while **6** was stable only in the A form of the DNA.

ESR Measurements.—Thin DNA filaments (outer diameter ≤ 0.4 mm) containing metalloporphyrins were placed into parallel holes (inner diameters 0.5 mm) made in a flattened surface of a quartz rod (outer diameter 4 mm). The quartz rod with DNA fibres was kept for more than 24 h at room temperature in an atmosphere of appropriate relative humidity, which was controlled by the vapour pressures of saturated aqueous solutions of an appropriate inorganic salt.[31,35] Then the quartz rod was attached to a goniometer head for the ESR measurement. The spectra were measured on a JEOL FE2XG X-band spectrometer at room temperature and at −150 °C, and on a Varian E.12 spectrometer at 30 K. The B-form DNA fibres on the goniometer were bathed with nitrogen gas of appropriate humidity so that they did not dry out during the measurement.

Simulation of spectra. The resonance magnetic field was calculated by a spin Hamiltonian (1) where *B* is the magnetic

$$H = B\cdot g\cdot S + \sum_i S\cdot A_i\cdot I_i \quad (1)$$

field vector, *g* is the *g* tensor of a metalloporphyrin, and A_i is the hyperfine interaction tensor of the *i*th nucleus in the complex; *S* and I_i are the electron- and nuclear-spin angular momentum operators, respectively.

The coordinate systems used for the calculation of the ESR line shapes are defined in Fig. 1(*a*)–1(*c*). The *Z* axis of the laboratory coordinate system (*X*, *Y*, *Z*) in Fig. 1(*a*) is parallel to the magnetic field *B*, and the *X* axis is parallel to the rotation axis of the quartz rod. The DNA fibre axis Z_f is in the *YZ* plane and Φ is the angle between the fibre axis Z_f and the magnetic field *B*. The X_f axis in the DNA fibre coordinate system (X_f, Y_f, Z_f) coincides with the *X* axis of the laboratory system. The coordinate system (X_g, Y_g, Z_g) in Fig. 1(*b*) represents the principal axis system of the *g* tensor of the metalloporphyrins. The Eurelian angles α, β and γ define the orientation of the *g* tensor in the DNA fibres; α is measured from the X_f axis, β is an angle between the DNA fibre axis and the g_z axis, and γ determines the orientations of the g_x and g_y axes. The direction of the static magnetic field *B* in the coordinate system (X_g, Y_g, Z_g) is also represented by the polar coordinates θ and ψ as shown in Fig. 1(*c*).

The ESR spectra were simulated by the numerical integration (2), $S(B_0)$ is the ESR absorption intensity at a magnetic field B_0 and $F(B)$ is the derivative of a Gaussian function representing an ESR absorption shape for a single molecule as shown in equation (3). In the case of complexes **1**, **2**, **5** and **6** $S(B_0)$ is calculated for each of the copper, cobalt and nitrogen nuclear spin components. The relative intensities of the nine nitrogen superhyperfine structures for the copper complexes were taken as 1:4:10:16:19:16:10:4:1, respectively.

$$S(B_0) = \int_0^{\pi} d\alpha \int_0^{\pi} \sin\beta d\beta \int_{-\pi/2}^{\pi/2} F[B_0 - B(\alpha,\beta,\gamma,\Phi)] \times G(\beta_0 - \beta)G(\gamma_0 - \gamma)P(\alpha,\beta,\gamma,\Phi)\, d\gamma \quad (2)$$

$$F(B) = -[B/(\sqrt{2\pi}\Delta B^3)] \exp(-B^2/2\Delta B^2) \quad (3)$$

$$\Delta B^2 = \Delta B_x^2 \sin^2\theta\cos^2\psi + \Delta B_y^2 \sin^2\theta\sin^2\psi + \Delta B_z^2 \cos^2\theta \quad (4)$$

The parameter ΔB in equation (3) is the absorption linewidth of $F(B)$, and is approximated as in (4), where ΔB_x, ΔB_y and ΔB_z have their usual meanings. The linewidth of each hyperfine component of the cobalt complexes was represented as a function of the magnetic quantum number m_I ($\pm\frac{7}{2}$, $\pm\frac{5}{2}$, $\pm\frac{3}{2}$, $\pm\frac{1}{2}$) of the transition as in equation (4b)[36] where ΔB^0_i, a_i and b_i are the parameters to be adjusted.

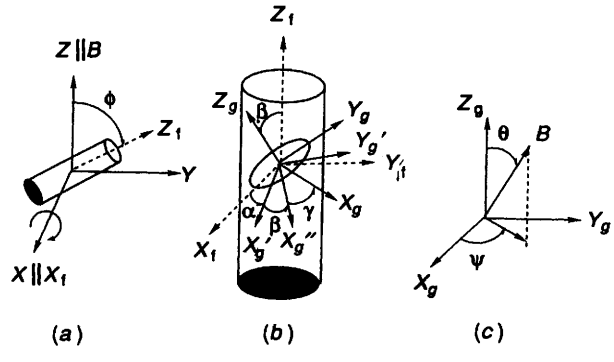

Fig. 1 Coordinate systems used for the calculation of ESR line shapes. (*a*) The orientation of the DNA fibre axis in the experimental coordinate system. The magnetic field *B* is taken as the *Z* axis. The fibre axis Z_f is rotated in the *YZ* plane. (*b*) The orientation of the principal axes (X_g, Y_g, Z_g) of the *g* tensor in the DNA fibre coordinate system (X_f, Y_f, Z_f); α, β and γ are the Eulerian angles connecting the (X_g, Y_g, Z_g) and (X_f, Y_f, Z_f) systems. Rotation of X_f and Y_f by α around the Z_f axis gives X_g' and Y_g' axes. The coordinate system (X_g', Y_g', Z_f) is transformed into (X_g'', Y_g', Z_g) with a rotation by β around the Y_g' axis. Finally, a rotation of (X_g'', Y_g', Z_g) by γ around the Z_g axis gives the (X_g, Y_g, Z_g) system. (*c*) The direction of the static magnetic field *B* in the *g* tensor coordinate system

$$\Delta B_i = \Delta B^0{}_i + a_i(m_I - b_i)^2; \quad (i = x, y \text{ and } z) \quad (4b)$$

The parameter $B(\alpha,\beta,\gamma,\Phi)$ in equation (2) is the resonance magnetic field of the complex the orientation of which with respect to the fibre axis is represented by α, β and γ, $G(\beta - \beta_0)$ and $G(\gamma - \gamma_0)$ are Gaussian distribution functions for angles β and γ centred at β_0 and γ_0 with standard deviations $\Delta\beta$ and $\Delta\gamma$, respectively. The term $G(\beta - \beta_0)$ is given in equation (5). Angle

$$G(\beta - \beta_0) = -\frac{1}{\sqrt{2\pi}\Delta\beta} \exp[-(\beta - \beta_0)^2/(2\Delta\beta^2)] \quad (5)$$

α is assumed to be completely random. Therefore, the g_z axis lying on the surface of the cone defined by β is equally probable for any α. The parameter $P(\alpha,\beta,\gamma,\Phi)$ in equation (2) is the anisotropic transition probability expressed by equation (6),[37] which can be transformed as a function of α, β, γ and Φ. The

$$P(\alpha,\beta,\gamma,\Phi) = [g_x^2 g_y^2(1 - \cos^2\theta) + g_y^2 g_z^2(1 - \sin^2\theta\cos^2\psi) + g_z^2 g_x^2(1 - \sin^2\theta\sin^2\psi)]/g^3 \quad (6)$$

$$g = (g_x^2\sin^2\theta\cos^2\psi + g_y^2\sin^2\theta\sin^2\psi + g_z^2\cos^2\theta)^{\frac{1}{2}} \quad (7)$$

resonance magnetic fields for the copper or cobalt complexes were calculated by perturbation methods to second order for the copper or cobalt hyperfine interaction and to first order for the nitrogen superhyperfine interactions using an axially symmetric spin Hamiltonian in which $g_x = g_y = g_\perp$, $g_z = g_\parallel$, $A_x = A_y = A_\perp$ and $A_z = A_\parallel$.

Molecular Modelling.—The binding structures of the porphyrins were also examined by use of the three-dimensional graphics software system BIOGRAF[38] run on a TITAN 3000 workstation.

Results and Discussion

Complex $[CuL^1]Cl_4$ **1**.—To examine the validity of our experimental method, we measured first the ESR spectra of complex **1** which has already been established to bind by an intercalative process to the DNA double helix.[4,23] Figs. 2(*a*) and 3 show the observed spectra for **1** on the A- and B-form DNA fibres prepared under low (≈60%) and high (≈95%) relative humidities, respectively. Under both conditions, the intense $g_\parallel$ components observed at $\Phi = 0°$ become considerably weak at $\Phi = 90°$, whereas the intensity of the $g_\perp$ components around 320 mT is at a maximum at $\Phi = 90°$. These results clearly indicate that there is a considerable amount of the intercalated species the porphyrin planes of which in the DNA fibres are almost perpendicular to the DNA fibre axis. The weak signal at $\Phi = 90°$ in the $g_\parallel$ region and the relatively intense 'extra-hyperfine' signal around 330 mT observed both at low and high humidity indicate that the observed spectra may not be due only to the intercalated species. As shown in Fig. 2(*b*), the observed spectra of **1** on A-form DNA fibres were reproduced assuming 80% of the complex is bound by intercalation and the other 20% is bound randomly on the DNA. Similar spectra were obtained also by assuming that the non-intercalated species are bound in the groove with the porphyrin plane tilted by about 45°. In both cases, the β_0 and $\Delta\beta$ values for the intercalated species were estimated as 10 and 20° respectively. Thus, it was difficult to determine whether the non-intercalated species of **1** are randomly oriented on DNA or stereospecifically oriented in the groove.

The ratio of the amount of the intercalated to that of the non-intercalated species changes with preparation conditions for the DNA fibres, particularly with the relative humidity. It has been reported that the binding mode of complex **1** to DNA depends on the ionic strength of the DNA solutions.[6,23] The electrostatic interaction between the cationic porphyrins and the anionic phosphoester groups of the DNA becomes effective at low ionic strength, and the porphyrins tend to bind on the surface of the DNA double helices. Therefore, the observation of more intense $g_\parallel$ and extra-hyperfine signals at $\Phi = 90°$ at higher relative humidity (Fig. 3) indicates an increased fraction of non-intercalated species. The linewidths of the ESR spectra, shown in Fig. 3, of complex **1** on the B-form DNA become very narrow, *i.e.* superhyperfine splittings emerged on the low-field $A_\parallel$ component of the spectra observed at $\Phi = 0°$ and on the so-called extra-hyperfine component observed at the high-field end of the spectrum at $\Phi = 90°$. The ^{31}P NMR spectra of various DNA fibres have revealed that the freedom of rotational motion of the DNA double helix about the helical axis remains at high humidity.[31] The observed sharpening of the spectra is attributed, therefore, to the motional averaging of the inhomogeneous environment around the complex.

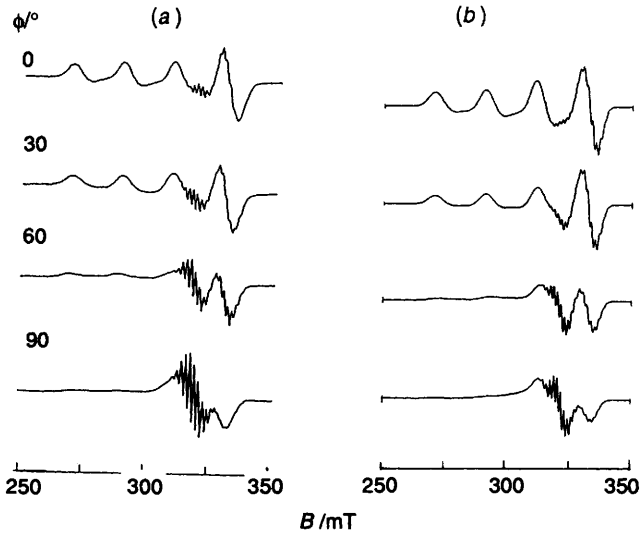

Fig. 2 Observed (*a*) and calculated ESR spectra (*b*) of complex **1** on A-form DNA fibres at room temperature. Microwave frequency: 9189 MHz, microwave power 10 mW, field modulation amplitude 5 G (1 G = 10^{-4} T). Magnetic parameters used for the simulation: $g_\parallel$ = 2.185, $g_\perp$ = 2.05, $A_\parallel$ = 0.0204 cm^{-1}, $A_\perp$ = 0.0029 cm^{-1}, $A_{N\parallel} = A_{N\perp}$ = 0.0015 cm^{-1}, $\Delta B_\parallel$ = 14 G, $\Delta B_\perp$ = 12 G, β_0 = 10° and $\Delta\beta$ = 20°; 20% of the complex was assumed to be randomly oriented on the fibres

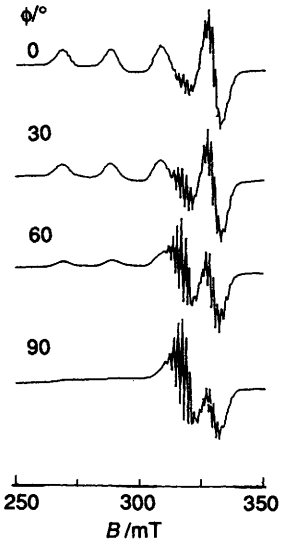

Fig. 3 Observed ESR spectra of complex **1** on B-form DNA fibres at room temperature. Microwave frequency 9186 MHz, microwave power 10 mW, field modulation amplitude 5 G

One should note that the single crystal-like ESR patterns observed in the $g_{\|}$ region of the spectrum at $\Phi = 0°$ for A-form DNA at low relative humidity deform toward bell-shaped ones at high relative humidity. This also indicates that a decrease in the ionic strength causes some of complex **1** to come out of the intercalation site, resulting in an increase in the amount of non-intercalated species. It is well known that DNA double helices adopt the B form at high relative humidity (>95%) and the A form at low relative humidity (<75%).[31] The average planes of the hydrogen-bonded base pairs in the B-form DNA are almost perpendicular to the helix axis, while those in A-form DNA tilt by about 20° from the plane perpendicular to the helix axis. If **1** intercalates between the base pairs in A-form DNA the porphyrin plane might also tilt about 20° along with the base pairs. However, the estimated angle of $\beta_0 = 10°$ for the intercalated species at low humidity is much smaller than the angles expected for A-form DNA. It has been observed that the intercalation of a flat aromatic molecule tends to fix the tertiary structure of DNA around the binding site in the B form.[8] Our result is consistent with this.

Complex $[CuL^2]Cl_4$ **2**.—The orientation dependence of the ESR spectra of complex **2** on the B-form DNA fibres shown in Fig. 4(*a*) differs considerably from that of **1**. The intensities of the two hyperfine peaks observed around 270 and 290 mT increase with increasing Φ to a maximum at about $\Phi = 30°$. This result clearly indicates that **2** has a specific orientation with respect to the DNA helix axis. The observed ESR spectra were reproduced with $\beta_0 = 45°$ and $\Delta\beta = 20°$ as shown in Fig. 4(*b*).

Doughty *et al.*[23] have measured ESR spectra of complex **1** on a film of calf thymus DNA, and showed that the complex intercalates to the DNA. Since the orientations of the DNA double helices are random in the film plane and the porphyrin planes of **2** are not perpendicular to the DNA helical axis, one cannot estimate the angle between the porphyrin plane and the helical axis from the ESR spectra of the complex in the film. Thus, our DNA-fibre ESR technique has an advantage for estimating the tilt angle of the porphyrin planes on the DNA double helices.

Complex **2** on the A-form DNA gave the ESR spectra with a weaker Φ dependence compared with those of B-form DNA.

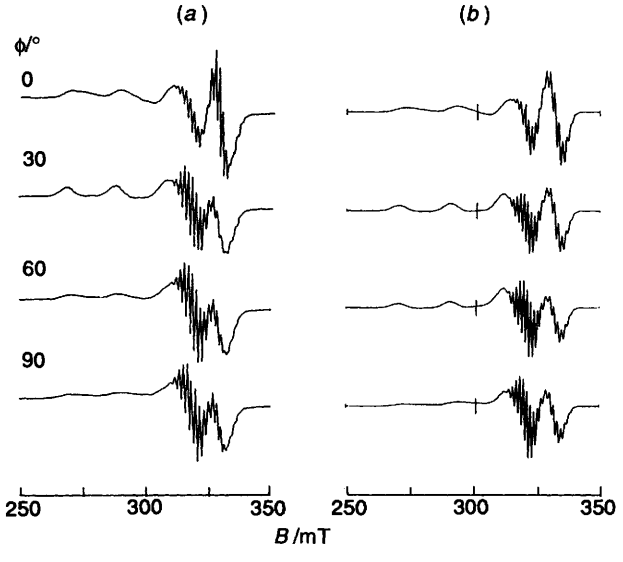

Fig. 4 Observed (*a*) and calculated ESR spectra (*b*) of complex **2** on B-form DNA fibres at room temperature. Microwave frequency: 9195 MHz, microwave power 10 mW, field modulation amplitude 5 G. Magnetic parameters used for the simulation: $g_{\|} = 2.180$, $g_{\perp} = 2.05$, $A_{\|} = 0.0204$ cm^{-1}, $A_{\perp} = 0.0027$ cm^{-1}, $A_{N\|} = 0.0015$ cm^{-1}, $A_{N\perp} = 0.0013$ cm^{-1}, $\Delta B_{\|} = 14$ G, $\Delta B_{\perp} = 10$ G, $\beta_0 = 45°$ and $\Delta\beta = 20°$

This suggests that the fluctuation of the orientations of the porphyrin planes increases with decreasing relative humidity. In the preparation of the DNA fibres, **2** binds first to B-form DNA in the solution, and then the DNA changes gradually to the A form during the fibre drying process. The minor groove in A-form DNA is considerably wider and shallower than that in B-form DNA. Such a deformation of the minor groove during the conformation change may cause a fluctuation in the orientation of **2** on the DNA fibres if it binds to the minor groove of DNA. Besides the structural change of the DNA, **2** has several geometrical isomers with respect to the directions of the 2-*N*-methylpyridyl groups. This may also cause the orientation of the porphyrin plane to fluctuate on the DNA fibre.

Complex $[FeCl(L^1)]Cl_4$ **3**.—This cationic complex binds very strongly to DNA. Mixing the complex and the DNA solution in the same complex : base pair ratio as in the case of the copper(II) complex caused DNA to precipitate. This is due to cross-linkage between the DNA double helices through the cationic *N*-methylpyridyl groups and/or the central iron(III) ions. The observed ESR spectra of this complex on A-form DNA fibres at −150 °C are shown in Fig. 5(*a*). In this case the intensity of the $g_{\perp}$ peak at around 100 mT increases with increasing Φ and reaches a maximum at around $\Phi = 60°$. This also indicates that the $g_{\|}$ axis is not parallel to the DNA fibre axis. The observed spectra were reproduced with $\beta_0 = 45°$ and $\Delta\beta = 20°$ as shown in Fig. 5(*b*). On the other hand, the ESR spectra observed for the B-form DNA fibres at −150 °C did not show any conspicuous angular dependence. The freezing of the B-form DNA fibres might result in the disruption of the orientations of the helical axes and/or porphyrin planes in the fibres.

According to Ward *et al.*,[10,11] complex **3** binds to the AT sites in the minor groove. However, the estimated β value of 45° is much smaller than that expected for the complex bound to the broad and shallow minor groove of A-form DNA. It should also be noted that the estimated Δβ value of 20°, representing the fluctuation of the porphyrin planes, is equal to that of **2** on the B-form DNA fibres. These results suggest that **3** binds so strongly to the B-form DNA double helix that the tertiary structure of the neighbourhood of the binding site cannot rearrange with changing relative humidity.

Bis(imidazole) Adduct $[FeCl(L^1)(Him)_2]Cl_4$ **4**.—In contrast to **3**, the binding of complex **4** to DNA does not cause DNA

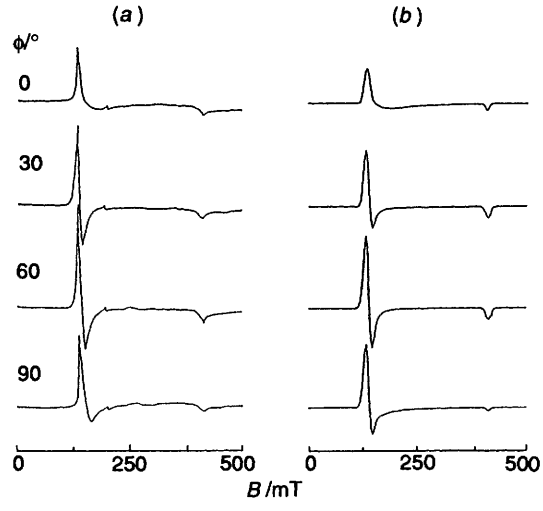

Fig. 5 Observed (*a*) and calculated ESR spectra (*b*) of complex **3** on A-form DNA fibres at −150 °C. Microwave frequency 9180 MHz, microwave power 10 mW, field modulation amplitude 5 G. Magnetic parameters used for the simulation: $g_{\|} = 6.00$, $g_{\perp} = 2.00$, $\Delta B_{\|} = 60$ G, $\Delta B_{\perp} = 60$ G, $\beta_0 = 45°$ and $\Delta\beta = 20°$

precipitation. The difference can be attributed to shielding of the central iron(III) ion with the two imidazole groups which interfere with cross-link formation. It was also observed that the low-spin dicyano-derivatives of **3** do not bind to DNA. In spite of the 4+ charge remaining on the *N*-methylpyridyl groups, the negative charge around the $Fe^{III}(CN)_2$ moiety inhibits the binding of this complex to the DNA. Thus the positive charge around the iron(III) site in the porphyrin plays a critical role in the binding of the porphyrin itself as well as in cross-link formation.

As shown in Fig. 6, the ESR spectrum of complex **3** with an excess of imidzole in frozen solution reveals two kinds of low-spin species, with $g_z = 2.85$ and $g_x = 1.60$ (a) and $g_z = 2.73$ and $g_x = 1.74$ (b). The g values of b are similar to those ($g_z = 2.70$, $g_y = 2.21$, $g_x = 1.69$) of haemoglobin histidine in which the imidazole N^1 is deprotonated.[39]

Fig. 7(*a*) shows the changes in the ESR spectra with Φ for complex **4** on the A-form DNA fibres at 25 K. The g values are of the type a observed in the frozen solution. Fig. 7(*b*) shows the calculated spectra with $\beta_0 = 90°$, $\Delta\beta = 40°$, $\gamma_0 = 0°$ and $\Delta\gamma = 50°$. Though adsorbed dioxygen, high-spin iron(III) species and other paramagnetic impurities on the DNA fibres distorted the line shapes, the observed peak positions and the orientation-dependent relative intensities were well reproduced.

The orientations of the principal axes of the g tensor in the low-spin iron(III) porphyrins have been extensively investigated; the g_z axis is perpendicular to the porphyrin plane, and the g_x and g_y axes are in the porphyrin plane.[40–43] Though the orientation of the g_x axis is not so well documented as the g_z axis, it is usually taken as perpendicular to the co-ordinating imidazole plane. These assignments for the orientations of the

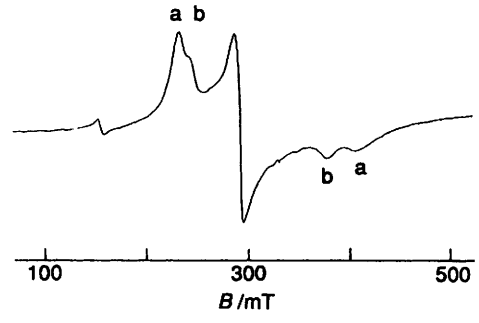

Fig. 6 The ESR spectrum of complex **3** with an excess of imidazole (giving **4**) in frozen aqueous solution at 25 K. Microwave frequency 9176 MHz, microwave power 5 mW, field modulation amplitude 5 G

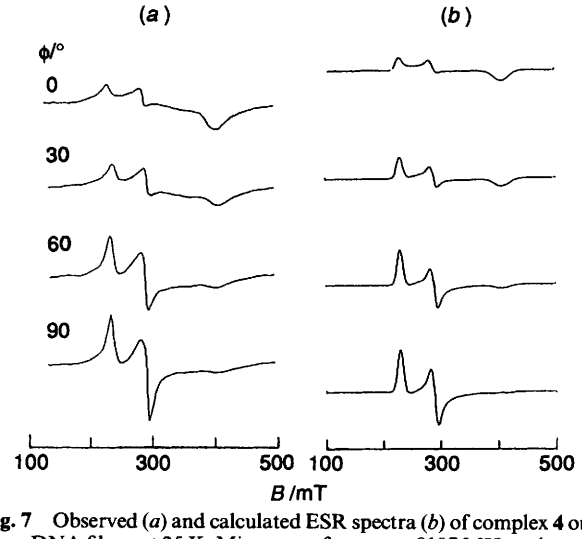

Fig. 7 Observed (*a*) and calculated ESR spectra (*b*) of complex **4** on A-form DNA fibres at 25 K. Microwave frequency 9187 MHz, microwave power 5 mW, field modulation amplitude 5 G. Magnetic parameters used for the simulation: $g_x = 1.60$, $g_y = 2.26$, $g_z = 2.84$, $\Delta B_x = 50$ G, $\Delta B_y = 60$ G, $\Delta B_z = 100$ G, $\beta_0 = 90°$, $\Delta\beta = 40°$, $\gamma_0 = 0°$ and $\Delta\gamma = 50°$

g-tensor axes in the molecular frame suggest that the porphyrin planes are parallel and the imidazole planes are perpendicular to the fibre axis, though the fluctuations $\Delta\beta$ and $\Delta\gamma$ are large. A molecular modelling study indicates that two imidazole groups co-ordinated at the axial positions make the complex too bulky to bind deeply in a minor groove of B-form DNA. Though these results do not exclude the possibility of the complex binding in a major groove, the binding mode of this complex is reasonably classified as 'outside binding' by considering the average orientation and its large fluctuation of the porphyrin plane on the DNA.

Complex $[CoL^1][ClO_4]_4$ **5**.—The ESR spectra of complex **5** in frozen aqueous solution change considerably with addition of adenine, adenosine or AMP as shown in Fig. 8(*a*)–8(*d*), respectively. Similar changes were observed upon additions of other nucleotides, nucleosides or nucleic bases. The magnetic parameters estimated from the ESR spectra are in Table 1, including those of uracil derivatives. Since the unpaired electron in a low-spin cobalt(II) porphyrin is in the d_z^2 orbital, the axial co-ordination causes a large change in the ESR parameters, *i.e.* the stronger the axial co-ordination the smaller are the $g_\perp$, $A_\parallel$ and $A_\perp$ values and the larger the $g_\parallel$ values.[44] The

Table 1 The ESR parameters of complex **5** in frozen solutions at −150 °C

Solvent	$g_\parallel$	$g_\perp$	$10^4 A_\parallel$/cm^{-1}	$10^4 A_\perp$/cm^{-1}
Water + ethylene glycol	2.037	2.34	86	*
+ adenine	2.025	2.41	96	57
+ adenosine	2.010	2.42	116	66
+ 3′-AMP	2.007	2.45	116	86
+ uracil	2.027	2.42	95	57
+ uridine	2.007	2.43	110	66
+ 3′-UMP	2.013	2.41_5	109	62

* The hyperfine splitting was not resolved.

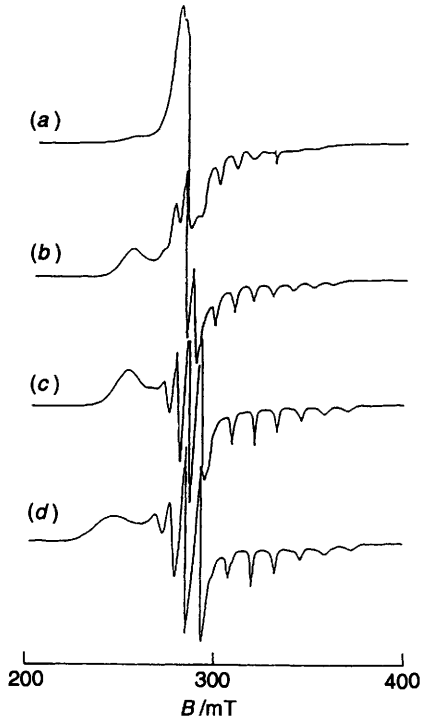

Fig. 8 The ESR spectra of complex **5** in frozen solutions at −150 C°: (*a*) Mol ratio water: ethylene glycol = 12 : 1; (*b*) (*a*) + adenine; (*c*) (*a*) + adenosine; (*d*) (*a*) + 3′-AMP. In (*b*)–(*d*), nucleic base: Co = 10 : 1. Microwave power 10 mW, field modulation amplitude 5 G

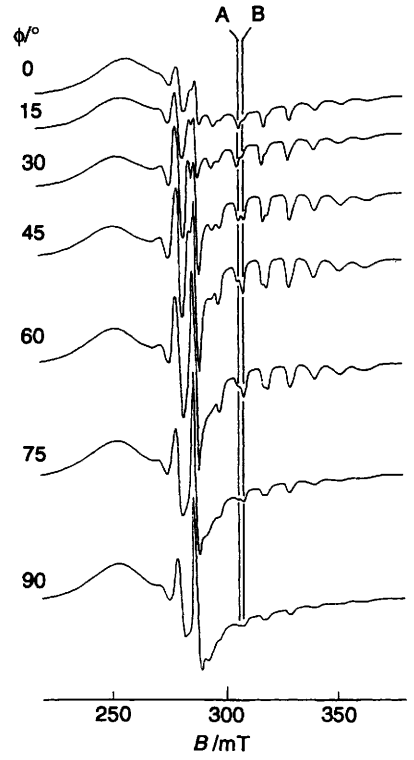

Fig. 9 The ESR spectra of complex **5** on A-form DNA fibres at −150 °C: A and B on the $m_I = \frac{3}{2}$ components correspond to the two different species with different hyperfine splitting constants

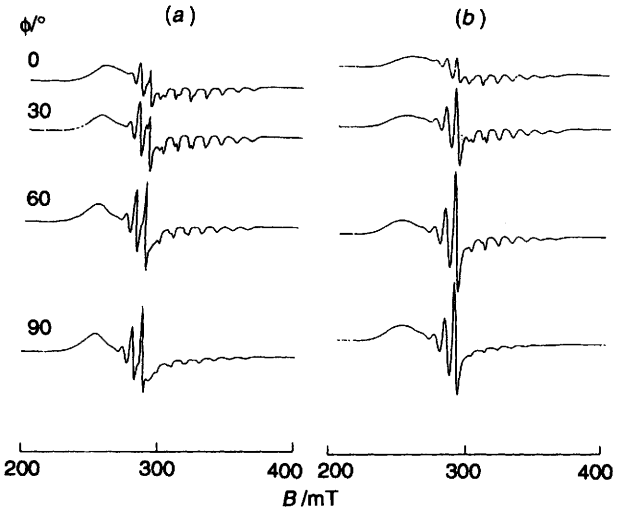

Fig. 10 Observed (*a*) and calculated ESR spectra (*b*) of complex **5** on B-form DNA fibres at −150 °C. Microwave frequency 9181 MHz, microwave power 10 mW, field modulation amplitude 5 G. Magnetic parameters used for the simulations: intercalated species, $g_{\|} = 2.030$, $g_{\perp} = 2.46$, $A_{\|} = 0.0109\ cm^{-1}$, $A_{\perp} = 0.0069\ cm^{-1}$, $\beta_0 = 10.0°$, $\Delta\beta = 25.0°$, $\Delta B°_{\|} = 16.0$ G, $a_{\|} = 200$, $b_{\|} = 1.5$, $\Delta B°_{\perp} = 20.0$ G, $a_{\perp} = 600$, $b_{\perp} = -3.6$; groove-bound species, $g_{\|} = 2.017$, $g_{\perp} = 2.480$, $A_{\|} = 0.0103\ cm^{-1}$, $A_{\perp} = 0.0075\ cm^{-1}$, $\beta_0 = 45.0°$, $\Delta\beta = 25.0°$, $\Delta B°_{\|} = 15.0$ G, $a_{\|} = 200$, $b_{\|} = 1.5$, $\Delta B°_{\perp} = 20.0$ G, $a_{\perp} = 600$, $b_{\perp} = -3.6$ ($a_{\|} = a_z$, $a_{\perp} = a_x = a_y$ and $b_{\|} = b_z$, $b_{\perp} = b_x = b_y$). The ratio of the amounts of the intercalated and groove-bound species was taken to be 1 : 2

observation that additions of nucleic bases or their derivatives increase $g_{\perp}$, $A_{\|}$ and $A_{\perp}$ values and decrease $g_{\|}$ indicates that molecular complexes are formed in the solutions, not because of apical co-ordination of a phosphate group in the nucleotides or that of nitrogen-containing bases in the purines or pyrimidines, but owing to the π–π stacking of the aromatic nucleic bases with the porphyrin ring.

Fig. 9 shows the ESR spectra of complex **5** on the A-form DNA fibres at −150 °C. It should be noted that some $g_{\|}$ cobalt(II) hyperfine components are further split into two. This unambiguously indicates that **5** binds to DNA with two different modes. Furthermore, the intensities of the two components change differently with Φ, *i.e.* the intensity of species A is at a maximum at $\Phi = 0°$ and minimum at $\Phi = 90°$, while that of species B is at a maximum at around $\Phi = 45°$. As the $g_{\|}$ axis of complex **5** is perpendicular to the porphyrin plane, these results suggest that species A is intercalated whereas species B is bound in the groove. The ESR spectra observed for the complex on B-form DNA fibres at −150 °C were almost the same as those for the A-form DNA fibres. In this case freezing of the B-form DNA fibres did not make the orientation of the porphyrin completely random. The sucrose which was added to prevent oxidation of **5** might also prevent disruption of the orientations of the DNA helical axes upon the DNA fibres.

The observed and calculated spectra for complex **5** bound to the B-form DNA fibres are shown in Fig. 10, where the β_0 values of species A and B were taken to be 10 and 45° respectively and the species ratio is assumed to be 1 : 2. Though the fittings of the calculated spectra with the observed ones in the $g_{\perp}$ ($A_{\perp}$) regions still remain to be improved, the observed orientation dependence around the $g_{\|}$ ($A_{\|}$) region was reasonably well reproduced by the above model. The mismatching in the $g_{\perp}$ ($A_{\perp}$) regions is attributed to the cobalt nuclear quadrupole term which enhances the forbidden transitions ($\Delta m_I \neq 0$) which we have neglected in the simulation. The β_0 value of species B is similar to those of complex **2** or **3** suggesting that it is bound in the minor groove of B-form DNA.

Unexpectedly, the $g_{\|}$ value of the intercalated species A is larger than those of the groove-bound species B and the molecular complexes of **5** and nucleic bases. The solvent molecules can access more easily the groove-bound species or molecular complexes with nucleic bases in the solution than the intercalated species. Therefore, the observed difference in the $g_{\|}$ values cannot be attributed simply to the co-ordination of the water molecule to Co^{II} in species A. The larger $g_{\|}$ and smaller $A_{\perp}$ values of species A should be explained by a tightly sandwiched arrangement with the base pairs and/or a deformation of the porphyrin plane incurred by the intercalation.

Monoimidazole Adduct $[CoL^1(Him)][ClO_4]_4$ **6**.—The ESR spectra of complex **5** on the A-form DNA fibres with an excess of imidazole shown in Fig. 11(*a*) are of the type in Fig. 8(*a*), and show three-line superhyperfine splitting of the $g_{\|}$ peaks indicating that only one imidazole can co-ordinate to the porphyrin on DNA. The observed angular dependence of the ESR spectra was reproduced with $\beta_0 = 45°$ and $\Delta\beta = 30°$ as shown in Fig. 11(*b*). This result indicates that **6** can bind in the groove with the orientation of the porphyrin plane similar to those of **3** and **5** (species B). On making the DNA fibres, imidazole solution was added after complex **5** had bound to DNA. Therefore, the present results show that even the intercalated species comes out of the binding site to form **6**, which is trapped in the groove. This process seems to be slow because a weak signal due to a small amount of **5** having no axial imidazole still remains in the low magnetic field region in Fig. 11(*a*). It should be noted that no signals from the bis(imidazole) adduct were detected. Once the monoadduct is trapped in the groove, co-ordination of the second imidazole is inhibited by the DNA. Though **6** in the dried DNA fibres does not react with oxygen, it is rapidly oxidized in B-form DNA fibres through the oxygenated form. Thus, oxygenation of the complex or the reaction of activated oxygen with DNA requires water molecules, and spaces for the oxygenation of the monoadduct is reserved at the apical positions of the porphyrins in the groove of B-form DNA.

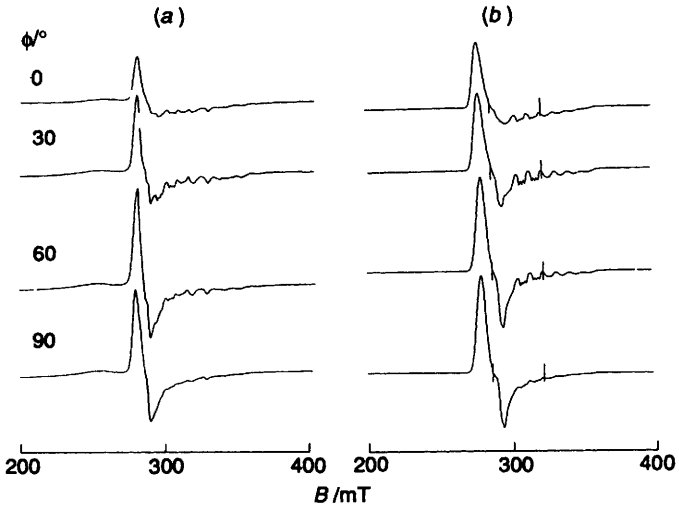

Fig. 11 Observed (*a*) and calculated ESR spectra (*b*) of complex **6** on A-form DNA fibres at −150 °C. Microwave frequency 9165 MHz, microwave power 10 mW, field modulation amplitude 5 G. Magnetic parameters used for the simulations: $g_{\|} = 2.030$, $g_{\perp} = 2.280$, $A_{\|} = 0.0085$ cm^{-1}, $A_{\perp} = 0.0017$ cm^{-1}, $A_{N\|} = 0.0019$ cm^{-1}, $A_{N\perp} = 0.0016$ cm^{-1}, $\beta_0 = 45.0°$, $\Delta\beta = 30.0°$, $\Delta B°_{\|} = 12.0$ G, $a_{\|} = 160$, $b_{\|} = 1.0$, $\Delta B°_{\perp} = 20.0$ G, $a_{\perp} = 50$, $b_{\perp} = -0.5$

Conclusion

The binding structures of complexes of Cu^{II}, Fe^{III} and Co^{II} of cationic water-soluble porphyrins on DNA were investigated by simulations of the ESR line shapes as a function of the orientations of DNA fibre with respect to the static magnetic field. The orientations of the bound porphyrins relative to the DNA helix axis change with the central metal ions, the substituent groups, and the axially co-ordinating groups in the porphyrins. The estimated geometrical parameters for the orientations of the porphyrins on DNA revealed clearly that the non-intercalative bindings are not always non-stereospecific ones. Complexes **2**, **3** and **6** bind in the groove with the normals of the porphyrin planes tilted about 45° from the double helix axes. Complex **4** is unique in that the porphyrin plane is almost parallel to the helix axis though the fluctuation of the porphyrin plane is large. The binding mode of this complex is reasonably classified as so-called 'outside binding'. Complex **5** was found to bind both in the intercalative and groove-bound modes. This result suggests that the non-intercalated species of **1** also binds with similar orientations in the groove. It was also revealed that some metalloporphyrins fix the DNA tertiary structures around the binding sites. Thus, ESR spectroscopy of the paramagnetic metalloporphyrins on DNA fibres was demonstrated to be a unique and advantageous technique to determine the orientations of the complexes and to probe the structure of the binding site.

Acknowledgements

M. C. would like to thank Dr. Hideo Kon for his useful discussions and encouragement during this work. He also acknowledges Professor Iwaizumi and Dr. Ohba of Tohoku University for measurement of ESR spectra at liquid-helium temperature.

References

1 R. J. Fiel, J. C. Howard, E. H. Mark and N. Datta-Gupta, *Nucl. Acid Res.*, 1979, **6**, 3093.
2 R. J. Fiel and B. R. Munson, *Nucl. Acid Res.*, 1980, **8**, 2835.
3 M. J. Carvlin, E. Mark, R. Fiel and J. C. Howard, *Nucl. Acid Res.*, 1983, **11**, 6141.
4 R. F. Pasternack, E. J. Gibbs and J. J. Villafranca, *Biochemistry*, 1983, **22**, 2406.
5 R. F. Pasternack, E. J. Gibbs and J. J. Villafranca, *Biochemistry*, 1983, **22**, 5409.
6 P. F. Pasternack, P. Garrity, B. Ehrlich, C. B. Davis, E. J. Gibbs, G. Orloff, A. Giartosio and C. Turano, *Nucl. Acid. Res.*, 1986, **14**, 5919.
7 E. J. Gibbs, M. C. Maurer, J. H. Zhang, W. M. Reiff, D. T. Hill, M. Malicka-Blaszkiewicz, R. E. Mckinnie, H.-Q. Liu and R. F. Pasternack, *J. Inorg. Biochem.*, 1988, **32**, 39.
8 R. E. Mckinnie, J. D. Choi, J. W. Bell, E. J. Gibbs and R. F. Pasternack, *J. Inorg. Biochem.*, 1988, **32**, 207 and the refs. therein.
9 J. M. Kelly, M. J. Murphy, D. J. McConell and C. OhUigin, *Nucl. Acid Res.*, 1985, **13**, 167.
10 B. Ward, A. Skorobogaty and J. C. Dabrowiak, *Biochemistry*, 1986, **25**, 6875.
11 B. Ward, A. Skorobogaty and J. C. Dabrowiak, *Biochemistry*, 1986, **25**, 7827.
12 D. L. Banville, L. G. Marzilli and W. D. Wilson, *Biochem. Biophys. Res. Commun.*, 1983, **113**, 148.
13 L. G. Marzilli, D. L. Banville, G. Zon and W. D. Wilson, *J. Am. Chem. Soc.*, 1986, **108**, 4188.
14 J. A. Strickland, D. L. Banville, W. D. Wilson and G. Marzilli, *Inorg. Chem.*, 1987, **26**, 3398.
15 J. A. Strickland, L. G. Marzilli, W. D. Wilson and G. Zon, *Inorg. Chem.*, 1989, **28**, 4191.
16 S. P. Greiner, R. W. Kreilick and L. G. Marzilli, *J. Bio. Str. Dyn.*, 1992, **9**, 837.
17 T. A. Gray, K. T. Yue and L. G. Marzilli, *J. Inorg. Biochem.*, 1991, **41**, 205.
18 J. H. Schneider, J. Odo and K. Nakamoto, *Nucl. Acid Res.*, 1988, **16**, 10323.
19 K. Bütje, H. Schneider, J.-J. P. Kim, Y. Wang, S. Ikuta and K. Nakamoto, *J. Inorg. Biochem.*, 1989, **37**, 119.
20 K. Bütje and K. Nakamoto, *J. Inorg. Biochem.*, 1990, **39**, 75.
21 R. Kuroda, H. Tanaka and S. Watanabe, *Nucleic Acids Symp. Ser.*, 1993, **29**, 123.
22 N. E. Geacintov, V. Ibanez, M. Rougee and R. V. Bensasson, *Biochemistry*, 1987, **26**, 3087.
23 G. Doughty, J. R. Pilbrow, A. Skorobogaty and T. D. Smith, *J. Chem. Soc., Faraday Trans. 2*, 1985, 1739.
24 G. Doughty, *J. Inorg. Biochem.*, 1988, **34**, 95.
25 F. R. Hopf and D. G. Whitten, *Porphyrins and Metalloporphyrins*, ed. K. M. Smith, Elsevier, 1975, ch. 16, p. 667.
26 B. Meunier, *Chem. Rev.*, 1992, **92**, 1411.
27 M. Chikira, W. E. Antholine and D. H. Petering, *J. Biol. Chem.*, 1989, **264**, 21478.
28 M. Chikira, T. Sato, W. E. Antholine and D. H. Petering, *J. Biol. Chem.*, 1991, **266**, 2859.
29 M. Chikira and Y. Mizukami, *Chem. Lett.*, **1991**, 189.
30 K. Sato, M. Chikira, Y. Fujii and A. Komatsu, *J. Chem. Soc., Chem. Commun.*, 1994, 625.
31 H. Shindo, J. B. Wooten, B. H. Pheiffer and S. B. Zimmerman, *Biochemistry*, 1980, **19**, 518 and the refs. therein.
32 D. Mauzerall, *The Porphyrins*, ed. D. Dolphin, Academic Press, 1978, vol. 5, p. 29.
33 R. J. Fiel, N. Datta-Gupta, E. H. Mark and J. C. Howard, *Cancer Res.*, 1981, **41**, 354.
34 N. Kobayashi, *Inorg. Chem.*, 1985, **24**, 3324.
35 F. E. M. O'Brien, *J. Sci. Instrum.*, 1948, **25**, 73.
36 R. Wilson and D. Kivelson, *J. Chem. Phys.*, 1966, **44**, 4445.
37 R. Aasa and T. Vanngard, *J. Magn. Reson.*, 1975, **19**, 308.
38 BIOGRAF, version 3.1, Molecular Simulation Inc., Waltham, MA, 1992.
39 R. Langridge, H. R. Wilson, C. W. Hooper, M. H. F. Wilkins and L. D. Hamilton, *J. Mol. Biol.*, 1960, **2**, 19.
40 D. A. Marvin, M. Spencer, M. H. F. Wilkins and L. D. Hamilton, *J. Mol. Biol.*, 1961, **3**, 547.
41 W. Fuller, M. H. F. Wilkins and L. D. Hamilton, *J. Mol. Biol.*, 1965, **12**, 60.
42 T. Otsuka, T. Ohya and M. Sato, *Inorg. Chem.*, 1987, **26**, 2191.
43 M. Sato, T. Otsuka and T. Ohya, *Nippon Kagaku Kaishi*, 1988, 522.
44 M. Kohno, K. Yamamoto, T. Sakurai and H. Ohya-Nishiguchi, *Bull. Chem. Soc. Jpn.*, 1984, **57**, 932 and refs. therein.

Received 30*th September* 1994; *Paper* 4/05982D